A Study of Miniaturization of Traveling Wave Direct Energy Converter for Loading on a Spacecraft

IEPC-2015-485p／ISTS-2015-b-485p

Presented at Joint Conference of 30th International Symposium on Space Technology and Science, 34th International Electric Propulsion Conference and 6th Nano-satellite Symposium
Hyogo-Kobe, Japan
July 4–10, 2015

H. Takeno[*], Y. Togo[†], T. Katsura[‡], and Y. Yasaka[§]
Kobe University, Kobe, Hyogo, 6578501, Japan

and

K. Ichimura[¶] and Y. Nakashima[‖]
University of Tsukuba, Tsukuba, Ibaraki, 3058577, Japan

Abstract: Traveling wave direct energy converter (TWDEC) was proposed as an efficient energy recovery device for fast protons produced by D-^{3}He fusion reaction. The application of TWDEC to fusion propulsion system was also studied, and its significant subject was miniaturization of the device. In TWDEC, there is a trade-off between device size and efficiency, and an employment of a decelerator of constant deceleration scheme is promising to realize miniaturization. The paper experimentally examines one of the working characteristics of the constant deceleration scheme by using a relative phase control method called active decelerator. The results of the experiment and corresponding numerical orbit calculation are consistent with the theory of the constant deceleration scheme.

Nomenclature

e	= unit charge
E	= ion energy
$\langle E \rangle$	= ion average energy
E_0	= extracted ion energy
f	= frequency of traveling wave
F	= energy distribution function
I_c	= collector current
m_i	= ion mass
q_i	= ion charge
v_0	= standard velocity of ion

[*]Professor, Department of Electrical and Electronic Engineering, takeno@eedept.kobe-u.ac.jp
[†]Graduate student, Department of Electrical and Electronic Engineering
[‡]Graduate student, Department of Electrical and Electronic Engineering
[§]Professor Emeritus, yasaka@kobe-u.ac.jp
[¶]Researcher, Plasma Research Center, ichimura_kazuya@prc.tsukuba.ac.jp
[‖]Director of Center, Plasma Research Center, nakashma@prc.tsukuba.ac.jp

V_0 = amplitude of voltages on the transmission line
V_{cnv} = beam convergence voltage
V_{dec} = deceleration voltage
V_{ex} = ion extraction voltage
V_{ir} = ion repeller grid voltage
V_{mod} = modulation voltage
λ = wavelength of traveling wave
ϕ_{c} = relative phase difference between V_{mod} and V_{dec} on numerical calculation
ϕ_{e} = relative phase difference between V_{mod} and V_{dec} on experiment
ϕ_{opt} = optimum relative phase difference between V_{mod} and V_{dec} on numerical calculation
θ_i = phases of voltages on the transmission line

I. Introduction

A traveling wave direct energy converter (TWDEC) was proposed as an energy recovery device for fast protons of 14.7 MeV created in D-^{3}He fusion reaction.[1,2] Usually, the length around one hundred meters are necessary for recovery of the fast protons by using a conventional electrostatic energy converter as the insulation length is needed to maintain high voltage of 14.7 MV. On one hand, the length of the TWDEC will be 20–30 meters, thus the compactness of the device is improved by using a TWDEC. Recently, TWDEC was proposed to be applied to a spacecraft.[3] In TWDEC, a part of energy of fast protons is converted into electric energy, and the protons with the remained energy are exhausted out of the TWDEC. These exhausted protons can be used for thruster of the spacecraft. In such a situation, TWDEC mounted on a spacecraft must be more compact than that in a terrestrial power plant, and miniaturization of TWDEC is required.

The TWDEC works based on the inverse process of a linear accelerator. The incident proton beam is velocity-modulated by a radio frequency (RF) field in the modulator. It is bunched in the downstream where the decelerator is settled. In the decelerator, a lot of grid electrodes are aligned in the direction of the beam, and the bunched beam induces RF current between the electrodes. The current flows in the external circuit and creates RF potential on the electrodes, by which deceleration field is formed between the electrodes. The field travels with the bunched beam in the beam direction, thus the protons are always in the deceleration field.

In TWDEC, there is a trade-off between device size and energy conversion efficiency. The main factor of the device size is the distance between the modulator and the decelerator, which is determined by bunching length in the modulation process. The bunching length can be shortened in a deep modulation, however, velocity deviation of the protons becomes large which results in a low conversion efficiency. In a shallow modulation, high efficiency can be expected with small velocity deviation whereas the bunching length becomes long. This trade-off must be considered for the miniaturization of TWDEC.

In the design of decelerator of TWDEC, the optimum deceleration scheme was often used.[4–6] In this scheme, the structure of the decelerator is determined by the motion of the proton with the standard incident velocity, thus protons with large velocity deviation degrade efficient deceleration. On one hand, the constant deceleration scheme was proposed,[7] in which protons were trapped in a potential valley of traveling wave and protons with large velocity deviation could be decelerated with bouncing motion in the valley. For miniaturization of TWDEC, velocity deviation becomes large to shorten the bunching length, thus the constant deceleration scheme is appropriate.

Experimental examinations of the constant deceleration scheme are not enough. The authors started an experimental study of the constant deceleration scheme.[8] In the previous paper, a decelerator was designed according to the theory of the constant deceleration scheme. The energy conversion efficiency over 30 % was obtained, which was the highest record in the experiment. In this paper, one of the working characteristics of the constant deceleration scheme is examined. The relation between the incident phase and deceleration characteristics is investigated by using an active decelerator. The results of the experiment are compared with the theory by referring the corresponding numerical orbit calculation. The purpose of the study is to show the consistency of the theory of the constant deceleration scheme.

The organization of the paper is as follows: the experiment on the constant deceleration scheme is shown in Section II. The corresponding orbit calculation and discussion referring the theory of the constant deceleration scheme are presented in Section III. The conclusion of the paper is given in Section IV.

II. Simulation Experiment

A. Experimental Device

We used an experimental simulator of TWDEC which is illustrated in Fig. 1. It consists of an ion source, a modulator, a decelerator, and a beam measurement system.

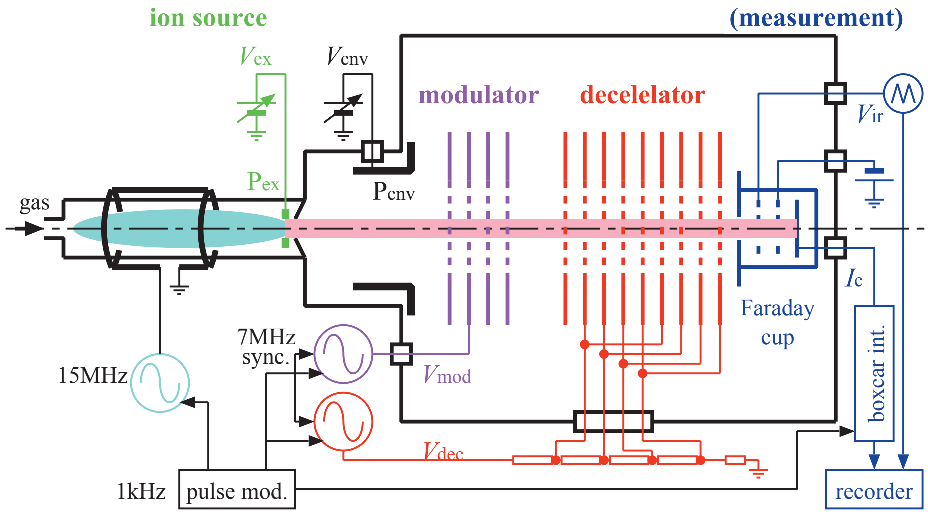

Figure 1. TWDEC experimental simulator.

An RF power of 15 MHz is supplied to an RF antenna of the ion source where helium gas is injected and a plasma is produced. The RF power is pulse-modulated, and the frequency of the pulse is 1 kHz and the duty is 50 %. The wall of the ion source is a glass tube, thus the plasma is floating electrically. By an application of high voltage to an extraction electrode (V_{ex}), helium ions with an energy of $E_0 = q_i V_{ex}$, where q_i is ion charge, are extracted to the metal chamber (helium ions instead of protons are used in the simulator). In the experiment of the present paper, 3.2 kV is used as V_{ex}, so the standard velocity of the ions is $v_0 = \sqrt{2E_0/m_i} = 3.9 \times 10^5$ m/s (m_i is ion mass). The velocity of individual ion distributes around v_0 due to plasma potential and ion thermal motion. The extracted ion beam is converged by an application of convergence voltage (V_{cnv}; usually 520 V) to a convergence electrode.

A number of circular-plate electrodes are aligned in the axial direction in the modulator and the decelerator. The arrangement of the electrodes is shown in Fig. 2, where electrode symbols are indicated. The helium ion beam can pass the center of the electrodes where stainless mesh are settled.

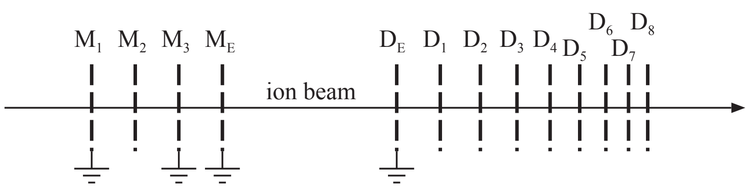

Figure 2. Arrangement of electrodes in the modulator and the decelerator.

The modulator consists of four electrodes. The modulation voltage (V_{mod}) is applied to the second electrode of M_2, and other electrodes (M_1, M_3, M_E) are grounded. In the experiment of the present paper, V_{mod} is 7 MHz in frequency (f) and 360 V_{0p} (V_{0p} means zero to peak voltage amplitude) in amplitude. The amplitude is modulated by a pulse signal synchronized with the pluse for plasma production RF in the ion source with an appropriate duty ratio. The intervals between the electrodes are taken to be 14 mm which corresponds to a quarter of the wavelength of the traveling wave ($\lambda/4 = v_0/4f$). In this condition, uniform electric fields are created between M_1 and M_2, and between M_2 and M_3. The extracted helium ions are velocity modulated by these electric fields.

In a practical TWDEC, deceleration voltage (V_{dec}) is induced by incident of bunched beam. In the present experiment, however, V_{dec} is externally supplied for examination of working characteristics of the decelerator. This is the same scheme as before[5,6,8] and is called *active decelerator*.

The decelerator consists of nine electrodes. The first electrode of D_E is grounded, and V_{dec} is applied to other electrodes (D_1–D_8). A dual channel generator supplies two signals of 7 MHz synchronized with each other, one of which is amplified and used as V_{mod}. The other is for V_{dec}, and also pulse-modulated and amplified in the same way as V_{mod}. The amplified output is supplied to a transmission line and voltages with the same amplitude and four different phases are obtained as $V_0 \exp(\mathrm{j}\theta_i)$ $(i = 1, ..., 4)$. The voltage $V_0 \exp(\mathrm{j}\theta_i)$ is applied to D_i and D_{i+4} $(i = 1, ..., 4)$. A traveling wave is created in the direction of the ion beam by taking $\theta_i - \theta_{i+1} = 90^\circ$ $(i = 1, 2, 3)$ when voltage of decelerator electrode is delayed with 90° than that of the former electrode. Some deviations remain on amplitude and phase in the used device, the detail of which is presented in the last paper.[8] By using this active decelerator system, phase difference between V_{mod} and V_{dec} (ϕ_{e}) is controlled by the dual channel generator with keeping constant phase differences among voltages on D_j $(j = 1, ..., 8)$. Note that ϕ_{e} does not necessarily mean the actual phase difference between V_{mod} and V_{dec} on electrodes. The phase difference at the signal generator is different from that between the electrodes because the lengths of the signal route are different. The values of ϕ_{e} in the following mean only as the relative one.

The beam measurement system consists of a Faraday cup (FCP), a bias controller, a boxcar integrator, and a signal recorder. The FCP has four mesh electrodes: a grounded cup, an ion repeller grid, a secondary electron suppressor grid, and a collector plate. The boxcar integrator samples and averages the collector plate current (I_{c}) by the pulse signal. By sweeping the ion repeller voltage V_{ir}, I_{c}–V_{ir} characteristic $I_{\mathrm{c}}(V_{\mathrm{ir}})$ is obtained. An energy distribution function of the beam can be derived according to the following equation:

$$F(E) \propto \frac{1}{\sqrt{V_{\mathrm{ir}}}} \frac{\mathrm{d}I_{\mathrm{c}}}{\mathrm{d}V_{\mathrm{ir}}}\bigg|_{V_{\mathrm{ir}}=\frac{E}{e}}. \tag{1}$$

The average energy can be obtained by

$$\langle E \rangle = \frac{\int_0^\infty EF(E)\mathrm{d}E}{\int_0^\infty F(E)\mathrm{d}E}. \tag{2}$$

B. Experimental Result

Figure 3 shows samples of measured energy distribution functions. The dashed curve shows the case without operation of TWDEC ($V_{\mathrm{mod}} = V_{\mathrm{dec}} = 0$ $\mathrm{V_{0p}}$) which means the incident beam. Note that ordinate value is reduced by 1/2. In this case, the most part of ions are around the extracted ion energy of $E_0 = q_{\mathrm{i}} V_{\mathrm{ex}} =$ 3.2 keV.

The solid curve shows the case with operation of TWDEC where $V_{\mathrm{mod}} = 360$ $\mathrm{V_{0p}}$ and the average amplitude of V_{dec} is 322 $\mathrm{V_{0p}}$. The ions are distributed in a wide energy range, especially a lot of distributions are found in the lower energy side than E_0. The average energy decreases due to operation of TWDEC.

According to Fig. 3, a considerable amount of distribution remains around E_0 even in the case with operation of TWDEC. This must be the result of the phenomenon reported previously. In the modulation experiment using a simple structure of the modulator as the present one, a phenomenon was observed that a significant part of the ions were not velocity-modulated.[9] Some possible reasons, such as field shielding by secondary electrons, were investigated, but the reason has not been clarified yet. So long as these ions are not velocity-modulated, they cannot be bunched, and thus enough deceleration effect cannot be expected. The remained component around E_0 in the case with operation of TWDEC in Fig. 3 must be the results of this.

The variation in $\langle E \rangle$ due to the phase difference between V_{mod} and V_{dec} (ϕ_{e}) was investigated. Figure 4 shows this result. According to Fig. 4, $\langle E \rangle$ roughly varies sinusoidally with ϕ_{e}. The best deceleration condition is $\phi_{\mathrm{e}} = 0.75\pi$, and the worst one is $\phi_{\mathrm{e}} = 1.75\pi$. This is because the deceleration of ions is due to trapping in the potential well of the decelerator field, and the shape of the well is roughly sinusoidal. The detailed discussion will be presented in the next section.

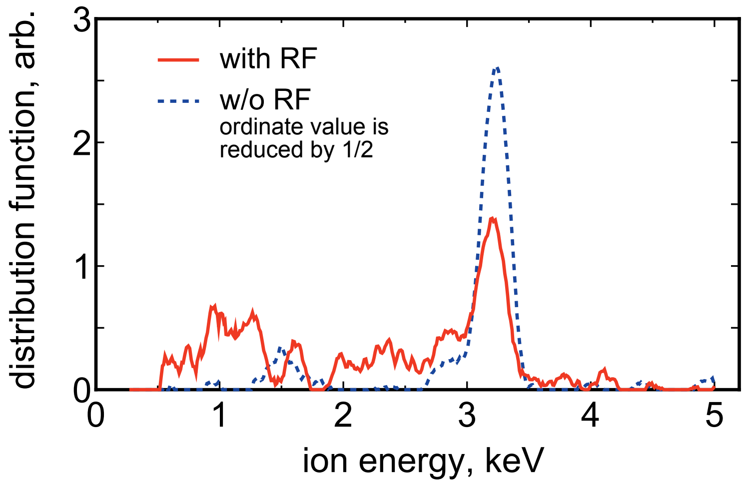

Figure 3. Variation of energy distribution function due to TWDEC operation.

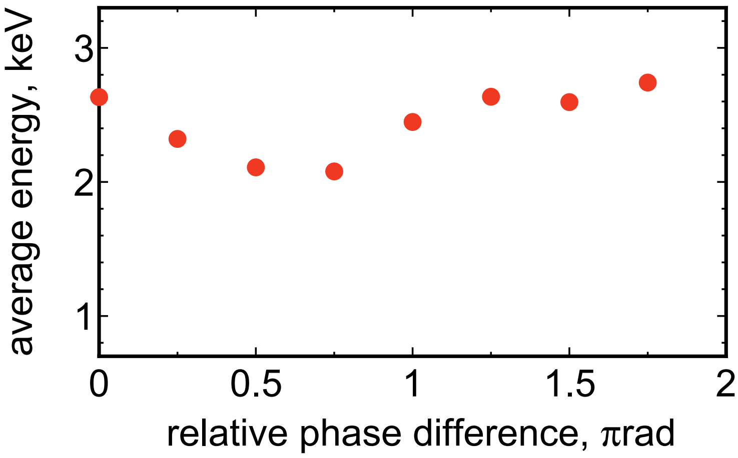

Figure 4. Variation in average energy to the phase difference between V_{mod} and V_{dec}.

For the cases of $\phi_e = 0.75\pi$ and 1.75π, energy distribution functions are shown in Figs. 5a) and Fig. 5b), respectively. In Fig. 5a), a lot of ions are found in the low energy region, especially a great peak around $E = 0.5$ keV which means ions are efficiently decelerated. On the other hand, there are considerable amount of ions are in the high energy region in Fig. 5b) as well as in the low energy region. The deceleration is not enough and some ions are accelerated. The deceleration effect is different contrastively according to the phase difference between V_{mod} and V_{dec}.

III. Orbit Calculation and Discussion

An ion orbit calculation corresponding to the simulation experiment was performed. The calculation model is one-dimensional (in the direction of the ion beam), and electric fields only by electrode potential are taken into account. The effect of particle charge does not introduced in the model. The same conditions of V_{ex}, V_{mod}, and V_{dec} as the experiment are used in the calculation. Energy distribution of the incident ions is also treated appropriately. The details of the calculation model are explained in Ref. 5.

Average energy of ions passing through the TWDEC can be evaluated also in the calculation. Average energies for eight kind of phase difference between V_{mod} and V_{dec} (ϕ_c) were examined, and the optimum phase difference (ϕ_{opt}) was obtained by taking ϕ_c for the lowest average energy case.

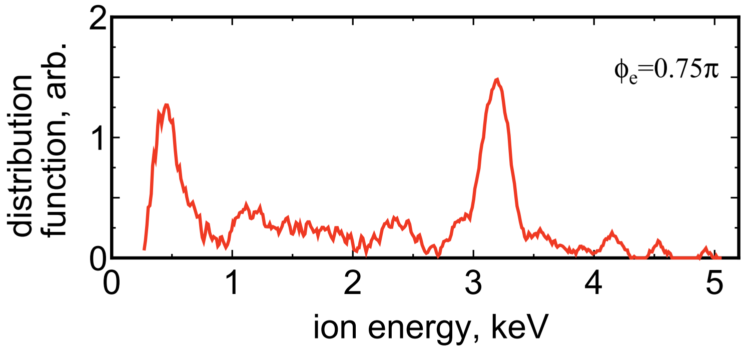

a)

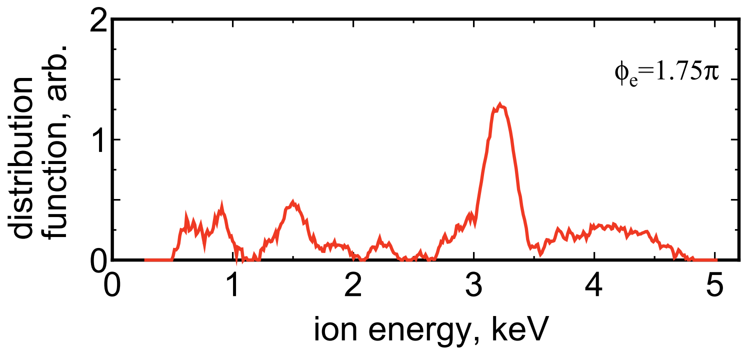

b)

Figure 5. Energy distribution functions for a) the best deceleration case ($\phi_e = 0.75\pi$) and b) the worst deceleration case ($\phi_e = 1.75\pi$).

Figure 6 shows energy distribution functions for the cases of a) $\phi = \phi_{opt}$ and b) $\phi = \phi_{opt} + \pi$. In Fig. 6a), the most part of the ions are in the low energy region less than 1 keV. On the other hand, significant distribution is found in the region over $E_0 = 3.2$ keV in Fig. 6b). These contrastive results are well corresponding to the experimental results in Fig. 5 although ions around E_0 are quite few which are considered as those are not velocity-modulated in the experiment. Except the remained component around E_0, the orbit calculation well reproduce the experimental result.

The deceleration characteristic is discussed by taking more detailed information from the calculation result. According to the theory of the constant deceleration, the ions trapped in the potential valley can be considered in a phase space diagram. Figure 7 shows an illustration of the phase space diagram for the constant deceleration, which expresses the condition of the ions when they are incident in the decelerator (arrive at the entrance of the decelerator). The abscissa is relative phase: zero and $\pm\pi$ correspond to the positions of bottom and top of the potential, respectively. The potential is that of traveling wave and its bottoms and tops are aligned periodically, thus their positions can be expressed by relative phase. The ordinate corresponds to velocity, and the horizontal center line means standard velocity v_0. The ions locating near the center of the diagram can be trapped and decelerated. The boundary of the trapping region is determined by the strength of the deceleration. Higher deceleration results in a narrower trapping region as shown in the figure. Qualitatively speaking, ions near the center of the diagram are highly possible to be trapped and decelerated.

The values of phase and velocity of ions at the entrance of the decelerator were taken in the numerical orbit calculation. The results are shown in Figs. 8a) and 8b) for the cases of $\phi_c = \phi_{opt}$ and $\phi_{opt} + \pi$, respectively. According to Fig. 8a), there are a lot of ions around the center of the diagram, so the ions are highly possible to be trapped, and thus, decelerated. As the case of $\phi_c = \phi_{opt}$ is the best deceleration condition, the result of Fig. 8a) is consistent with the constant deceleration theory. On the other hand, a few ions are near the center, and many ions far from the center in Fig. 8b). In this case, ions are highly possible to be untrapped. Actually, energy distribution for this case ($\phi_c = \phi_{opt} + \pi$) are as in Fig. 6b), and a few ions are distributed in the low energy region. The results of the numerical orbit calculation are quite consistent with the theory of the constant deceleration.

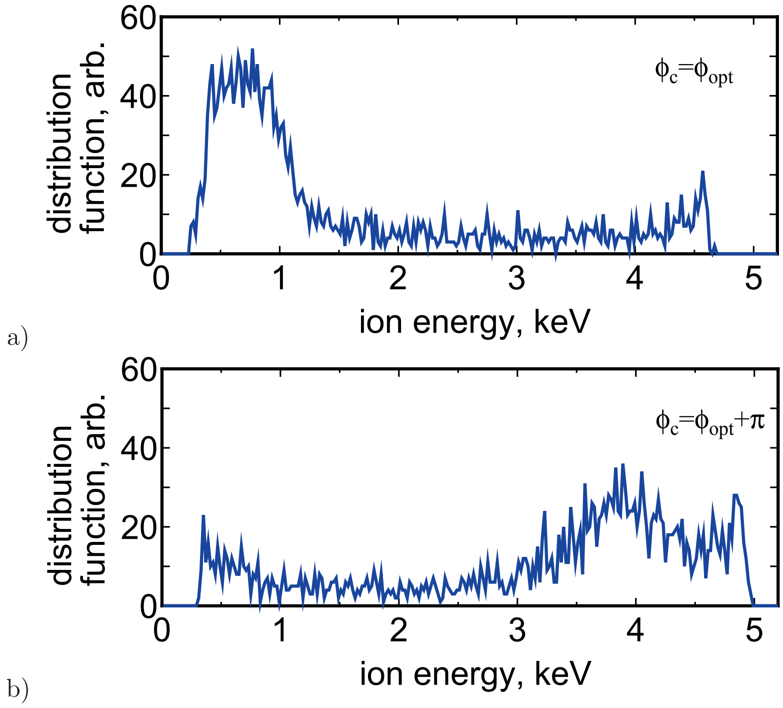

Figure 6. Calculated energy distribution functions for a) the best deceleration case ($\phi_c = \phi_{opt}$) and b) the case with the inverse phase ($\phi_c = \phi_{opt} + \pi$).

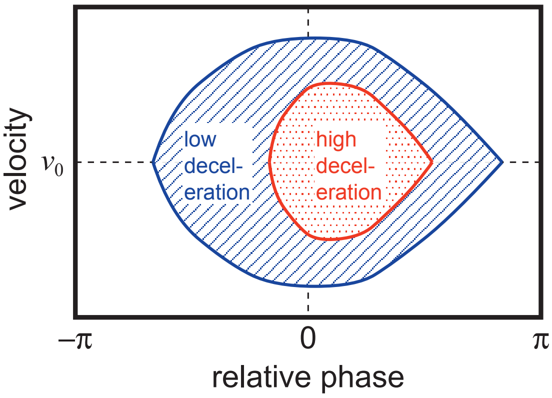

Figure 7. Phase space diagram for constant deceleration.

IV. Conclusion

The constant deceleration scheme in TWDEC was experimentally investigated by using active decelerator for miniaturization of TWDEC. The deceleration efficiency was varied according to relative phase difference between voltages of the modulator and the decelerator. A simple orbit calculation well reproduced the experimental result, and examination of ion distribution in the phase space showed a consistency of the results with the theory of constant deceleration scheme.

Acknowledgments

The authors acknowledge valuable discussions with Drs. J. Miyazawa, T. Goto, and I. Katanuma. This work was supported in part by the bilateral coordinated research between Plasma Research Center, University

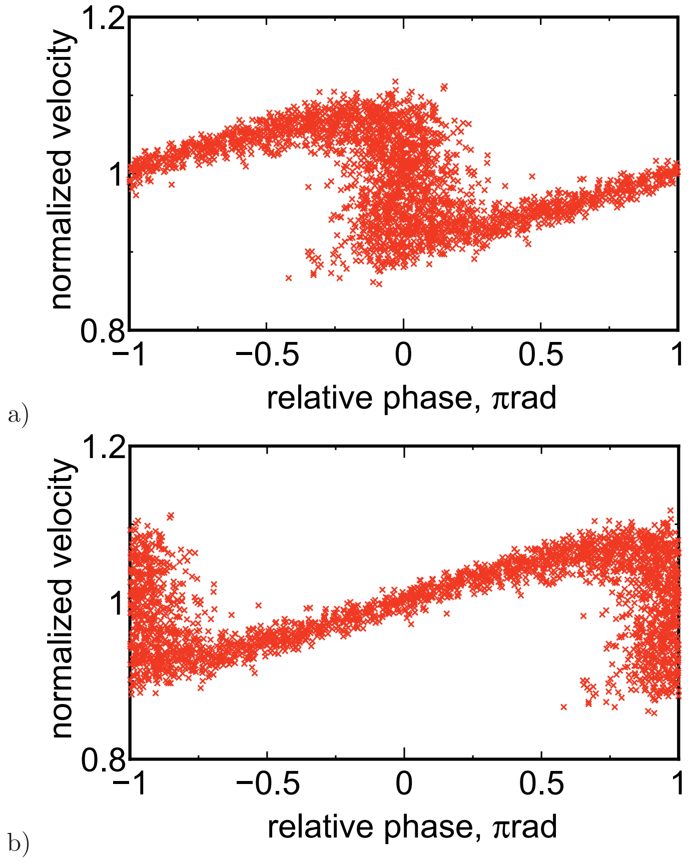

Figure 8. Phase space diagrams on velocity normalized by the standard velocity and relative phase obtained by orbit calculation in the cases of a) the best deceleration case ($\phi_c = \phi_{opt}$) and b) the case with the inverse phase ($\phi_c = \phi_{opt} + \pi$).

of Tsukuba, National Institute for Fusion Science, and Kobe University (NIFS13KUGM082).

References

[1] Momota, H., "Direct Energy Conversion of 15MeV Fusion Protons," Los Alamos Natl. Lab., LA-11808-C, May, 1990, pp. 8-13.

[2] Momota, H., Tomita, Y., Ishida, A., Kohzaki, Y., Ohnishi, M., Ohi, S., Nakao, Y., and Nishikawa, M., "D-^{3}He Fueled FRC Reactor ARTEMIS-L," *Proceedings of 14th International Conference on Plasma Physics and Controlled Nuclear Fusion Research*, 1992, IAEA-CN-56/G-13.

[3] Scott, J. H., George, J. A., and Tarditi, A. G., "Direct Energy Conversion for Low Specific Mass In-Space Power and Propulsion," *Proceedings of Nuclear and Emerging Technologies for Space 2013*, 2013, Paper 6756.

[4] Ishikawa, M., Kudo, T., Hayashi, S., Yamane, T., Tomita, Y., and Momota, H., "Basic Numerical Simulation of TWDEC for a D-^{3}He Fusion Reactor," *Fusion Engineering Design*, Vol. 41, 1998, pp. 541-546.

[5] Takeno, H., Ikeda, Y., Yamada, T., Noda, K., and Yasaka, Y., "Basic Experimental Simulation of a Traveling Wave Direct Energy Converter," *Japanese Journal of Applied Physics*, Vol. 39, Sept., 2000, pp. 5287-5291.

[6] Takeno, H., Yamamoto, T., Takada, K., Omoya, D., and Yasaka, Y., "Deceleration in a Traveling Wave Direct Energy Converter for Advanced Fusion," *Fusion Engineering Design*, Vol. 83, 2008, pp. 1696-1699.

[7] Katayama, H., and Sato, K., "Direct Energy Recovery from 15 MeV Fusion Protons by Using Traveling Waves," *Journal of Plasma and Fusion Research*, Vol. 77, No. 7, July, 2001, pp. 698-711 (in Japanese).

[8] Togo, Y., Katsura, T., Takeno, H., Yasaka, Y., Ichimura, K., and Nakashima, Y., "Experimental Study on the Constant Deceleration Scheme in Traveling Wave Direct Energy Converter," *Plasma and Fusion Research* [online journal], Vol. 10, 2015, 3405013, URL: http://www.jspf.or.jp/PFR/index.html [cited 15 May 2015].

[9] Fujita, F., Togo, Y., Takeno, H., Yasaka, Y., Ichimura, K., and Nakashima, Y., "Studies on Modulation Effect Analysis in Traveling Wave Direct Energy Converter," *9th Asia Plasma and Fusion Association*, Nov., 2013, TP-32.